ADVANCED FUNCTIONAL MATERIALS
www.afm-journal.de

Materials Views
www.MaterialsViews.com

Uniformly Interconnected Silver-Nanowire Networks for Transparent Film Heaters

*TaeYoung Kim, Yeon Won Kim, Ho Seok Lee, Hyeongkeun Kim, Woo Seok Yang, and Kwang S. Suh**

The fabrication and design principles for using silver-nanowire (AgNW) networks as transparent electrodes for flexible film heaters are described. For best practice, AgNWs are synthesized with a small diameter and network structures of the AgNW films are optimized, demonstrating a favorably low surface resistivity in transparent layouts with a high figure-of-merit value. To explore their potential in transparent electrodes, a transparent film heater is constructed based on uniformly interconnected AgNW networks, which yields an effective and rapid heating of the film at low input voltages. In addition, the AgNW-based film heater is capable of accommodating a large amount of compressive or tensile strains in a completely reversible fashion, thereby yielding an excellent mechanical flexibility. The AgNW networks demonstrated here possess attractive features for both conventional and emerging applications of transparent flexible electrodes.

1. Introduction

Transparent electrodes have been the focus of recent research, finding uses in applications including displays, touch-screen panels, and defrosting windows.[1–3] The most commonly used materials in these applications are indium-doped tin oxides (ITOs) owing to their high electrical conductivity and optical transmittance. However, ITO has certain limitations for use in next-generation devices: i) the increasing cost due to indium scarcity and processing requirements, which renders it difficult to use in low-cost, large-area electronics; ii) ITO is brittle and can easily wear out or crack when used in applications where bending is involved.[1–3]

To address these issues, recent work has devised strategies based on materials that have potential for large-area coverage and some degree of mechanical compliance. These materials include conducting polymers,[4,5] carbon nanotubes (CNTs),[6–8] graphenes,[9–11] metal grids,[12] and metallic nanowires.[13–17] The performance of these materials for applications as transparent electrodes is largely governed by two critical parameters: the surface resistivity and the optical transmittance. However, achieving low surface resistivity and high optical transmittance has been a challenge because these two values follow unfavorably opposing trends, and this often results in optoelectronic performances far inferior to those of ITOs.

Recently, silver nanowires (AgNWs) have emerged as one of the most-promising substitute for ITOs, because they offer optical transmittance and surface resistivity superior to their competitors.[13–22] Such use of AgNWs has been reported by many groups, including the possibilities for its use as transparent electrodes in optoelectronic applications.[13–22] De et al. demonstrated a method of producing AgNW films with an optical transmittance (T) of ≈85% and surface resistivity (R_s) of 13 Ω sq^{-1}.[14] Hu et al. reported solution-processed AgNW films with T = 80% and R_s = 20 Ω sq^{-1}.[15] Scardaci et al. demonstrated that AgNWs can be spray deposited over large areas to form networks with T = 90% and R_s = 50 Ω sq^{-1}.[17] However, previous work does not fully exploit the unique properties afforded by AgNW networks, indicating a lower electrical conductivity at a high transmittance region (>90%). Possible reasons for the limited performance of AgNW films include the relatively large diameter of AgNWs and the poor control over the network quality of AgNWs on the substrates, particularly when solution processes are used. Therefore, constructing uniformly connected networks of AgNWs with a small diameter is critical for improving the optoelectronic properties of AgNW-based electrodes and maximizing the potential of AgNW networks.

In this work, we present a method of preparing highly transparent, conductive, and flexible AgNW-based electrodes by controlling nanowire geometry and providing spatial uniformity of nanowire networks. For this purpose, we modified a solution-based synthetic method to prepare AgNWs with a small diameter and utilized exfoliated clay platelets as a key element to improve the solution and coating properties of AgNW inks, through which the nanowire networks are efficiently interconnected with improved spatial uniformity. Furthermore, we explore the use of uniform AgNW networks as a transparent electrode for film heaters. Film heaters have been the subject of research with a view to advancing a new type of automobile-window

Dr. T. Kim, Dr. H. Kim, Dr. W. S. Yang
Korea Electronics Technology Institute
68 Yatap-dong, Bundang-gu, Seongnam-si,
Gyeonggi-do 463-816, Korea
Y. W. Kim, H. S. Lee, Prof. K. S. Suh
Department of Materials Science and Engineering
Korea University
5-1 Anam-dong, Seongbuk-gu, Seoul 136-713, Korea
E-mail: suhkwang@korea.ac.kr

DOI: 10.1002/adfm.201202013

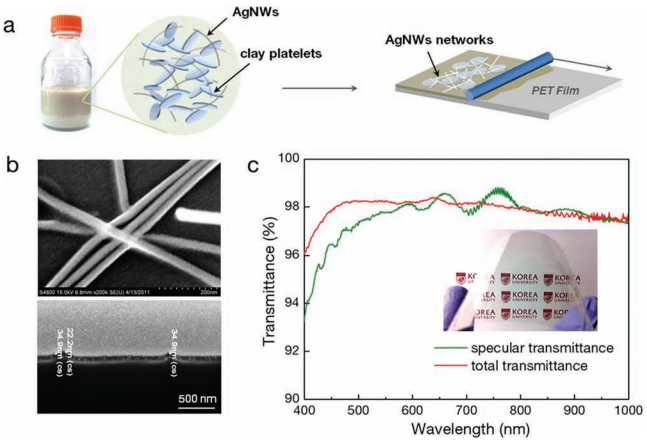

Figure 1. a) A schematic of the fabrication procedures for preparing transparent, flexible AgNW films by a wet-coating method. AgNW ink was prepared by dispersing AgNWs in water with a concentration of 5 mg mL^{-1} with clay platelets. (AgNW/clay ratio: 2/1 by weight). b) Top-view (upper) and cross-sectional (lower) scanning electron microscopy (SEM) images for as-synthesized AgNWs showing their diameter in the range of 20–40 nm. c) Total and specular optical transmission of the AgNW film with $R_s \approx 91\ \Omega\ sq^{-1}$ over the wavelength of 400–1000 nm.

defrosters and flexible outdoor panel displays.[23–25] Single-walled carbon nanotubes (SWNTs)[23] and graphene[24,25] have been demonstrated as transparent electrodes for film heaters: while they show a better performance than ITO films in terms of mechanical flexibility and rapid thermal responses, there are, however, several technical issues associated with their practical application, including the scalable processes for fabricating large-scale film heaters and the low operation voltage required for automobile window defrosters. Here, we demonstrate that optimally engineered AgNW-based films outperform other transparent conducting materials in that they show outstanding optoelectronic properties and enable rapid heating at low input voltages.

2. Results and Discussion

Figure 1a schematically illustrates our key process steps for producing highly conductive, transparent, and flexible films by coating AgNWs directly onto poly(ethylene terephthalate) (PET) films from a solution in water. Firstly, AgNWs were synthesized using a modified polyol process where AgNWs were produced through the reduction of $AgNO_3$ by ethylene glycol in the presence of poly(vinyl pyrrolidone) and 1-butyl-3-methylimidazolium chloride.[26–28] Modified synthetic methods gave access to the AgNWs with a relatively smaller diameter and a longer length, thereby achieving a high aspect ratio (>1000). The as-synthesized AgNWs had diameters of 20–40 nm and lengths up to 20–40 μm, as shown in the scanning electron microscopy (SEM) images (Figure 1b). Details for the AgNW synthesis are described in the Experimental Section. The AgNWs were washed, collected by centrifugation, and then re-dispersed in deionized water (≈5 mg mL^{-1}) with a dispersing agent, followed by the addition of synthetic clay made of nanometer-sized discotic platelets (diameter ≈ 25 nm and thickness ≈ 1 nm). While synthetic clays exist as agglomerates of stacked platelets in their dry form, they can be fully exfoliated and dispersed as separate clay platelets in water due to their hydrophilic nature.[29,30] The incorporation of clay platelets into a AgNW dispersion induced a uniform dispersal of the AgNWs in a network of fully exfoliated clay platelets. This process was typically accompanied by an increase in the solution viscosity, which is preferable for an optimally uniform AgNW coating. The as-formulated AgNW ink was then coated onto a 125 μm-thick poly(ethylene terephthalate) (PET) film using a wire-wound rod. The AgNW-coated film was produced by pulling a rod over the ink, while the wet-coating thickness was controlled by the ink concentration and the groove space in the wire-wound rod. This wet-coating process is scalable to an arbitrarily large area and compatible with the roll-to-roll coating process.

This enabled us to produce high-performance AgNW-based electrodes. By optimizing the nanowire network structure with the AgNW/clay ratio of 2/1 by weight, we produced solution-processed AgNW films with values of R_s = 91.3 Ω sq^{-1} and T = 97.9%, which surpassed the previously reported AgNW network.[13–22] This was achieved mainly by assembling thin AgNWs into large interconnected networks afforded by the incorporation of nanosized clay platelets. The high spatial uniformity of AgNW networks that we fabricated is corroborated by the small variation of surface resistivity measured at multiple locations. It is also noteworthy that the network quality could be improved by blending AgNWs with organic dispersing agents or a viscosity modifier, but this is typically accompanied by an unfavorable increase in the overall resistance of the nanowire film due to a high wire-wire junction resistance with the existence of electrically insulating molecules at the nanowire junction. However, the incorporation of clay nanoplatelets into the AgNW suspension was found to yield a minimal change in the resistance of the AgNW networks. This can be explained in that the silver nanowire junction was unlikely to be blocked by clay platelets due to the relatively small size (≈25 nm) of the separated clay platelets, and therefore the junction resistance would not be substantially affected at a AgNW/clay ratio of 2/1 (w/w). In addition, the clay coating itself conducts electricity by forming a contiguously interlinked and overlapping film of electrically charged platelets or absorbing moisture with the hydration of the ions within the layered crystal structure, thereby minimizing the change in the resistance of the AgNW film.

The specular optical transmittance (T) was measured with a UV–vis spectrometer using a blank substrate as the reference (i.e., without including the light absorbance of the substrate). Our AgNW film shows a high specular transmission over a wavelength in the visible and near-IR ranges (400–1000 nm) as shown in Figure 1c. The high optical-transmission value (97.7% @ 550 nm) achieved here is also attributed to the uniform network of thin and long AgNWs afforded by the exfoliated clay nanoplatelets. For comparison, the total transmission (T_t) data, which includes the light scattered by AgNWs, was also collected using an integrating sphere. From the difference in the total and specular transmission, the diffused light through the AgNW film was estimated to be less than 1%, confirming the clear visibility of the film with a low haze value.

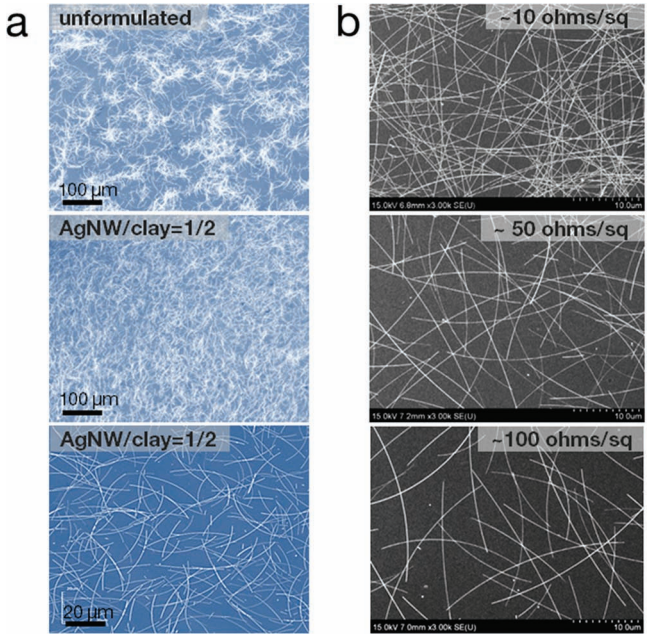

Figure 2. a) Top-view laser scanning microscopy (LSM) images of AgNW films derived from unformulated AgNW ink (uppermost) and formulated AgNW ink with clay platelets (middle). The bottom LSM image shows that AgNWs have a length up to 45 µm. b) Top-view SEM images of AgNW-coated films with different densities, in which the AgNWs are shown to be a continuous network.

The process described here allows reasonably good control over the morphology of AgNW networks, in a way that the AgNWs constitute an efficient electrical-conduction path across the film without a significant loss of optical transmittance. It is noteworthy that a coating of unformulated AgNW ink (without including clay platelets) causes self-aggregation of the AgNWs upon drying, leading to the uneven distribution of the nanowires (**Figure 2**a, top image). This phenomenon can be explained in the context of "coffee-ring" effects, in which the AgNWs are carried to the drying front of the wet film caused by the uncontrolled drying process.[31,32] We also note that the low viscosity of AgNW ink often leads to the breaking of the wet-coating layer into separated droplets on drying, which promotes the formation of unfavorably assembled AgNWs networks due to the uneven solvent evaporation of the droplets. Such self-aggregation has been greatly reduced in our AgNW film (Figure 2a, middle and bottom image), since the uniformly dispersed clay platelets in the ink prevent the uncontrolled assembly of AgNWs aided by the relatively high solution viscosity.

The density of the AgNW networks can be easily controlled by adjusting the concentration of the inks and the dimension of the wire-wound rod. Figure 2b presents a scanning electron microscopy (SEM) image of AgNWs deposited on PET films with different AgNW densities. The top-view images show that the AgNWs were interconnected with spatial uniformity over large areas. This continuous network provides electrical interconnects throughout the entire network with the formation of an effective percolative network. By increasing AgNW densities on the PET substrates, $R_s \approx 10\ \Omega\ sq^{-1}$ and $T \approx 90\%$ is achieved, which is sufficient for the use as transparent electrodes in diverse applications including transparent heaters, touch-screen panels, solar cells, and organic light-emitting diodes.

In general, the transmittance and surface resistivity for thin metallic films are expressed by

$$T(\lambda) = \left(1 + \frac{Z_0}{2R_s}\frac{\sigma_{op}(\lambda)}{\sigma_{dc}}\right)^{-2} \quad (1)$$

where Z_0 is the impedance of free space (377 Ω), R_s is the surface resistivity, $\sigma_{op}(\lambda)$ is the optical conductivity, and σ_{dc} is the DC conductivity of the film.[13,14]

The performance of an AgNW film can be rated using a figure of merit (FoM), which is taken as the ratio of the DC to optical conductivity, σ_{dc}/σ_{op}.[13,14] For high-performance electrode films, it is desirable to have a low surface resistivity and a high optical transmission, which corresponds to films with a high σ_{dc} and a low σ_{op}. The performance of the AgNW film was compared with other nanostructured materials including CNTs, graphene, and poly(ethylene dioxythiophene):poly(styrenesulfonate) (PEDOT:PSS), where specular optical transmittance is plotted against surface resistivity (**Figure 3**). Previous reports suggest that networks of AgNWs give a value of $\sigma_{dc}/\sigma_{op} \approx 400$,[13] which is much higher than those of other transparent conducting materials such as PEDOT:PSS (high-conductivity grade: $\sigma_{dc}/\sigma_{op} \approx 35$), single-walled CNTs (SWNTs) ($\sigma_{dc}/\sigma_{op} \approx 13$)[8] and graphene (doped CVD-graphene: $\sigma_{dc}/\sigma_{op} \approx 70$).[10] However, in case of previously reported AgNW films, theoretical predictions only apply to the data in the relatively low R_s region,[13] since the data deviates from the theoretical line for $R_s > 3\ \Omega\ sq^{-1}$ and $T > 80\%$ and displays a significantly lowered σ_{dc}/σ_{op} value in this industrially important region.

Our AgNW films display a σ_{dc}/σ_{op} of ≈300, close to the value measured for ITOs, and are best fitted with the theoretical prediction even at $R_s > 10\ \Omega\ sq^{-1}$ and $T > 90\%$. Because the transmittance and surface resistivity are directly related to the nanowire geometry and efficiency of the network formation, we attribute these improvements to the lowered wire diameter

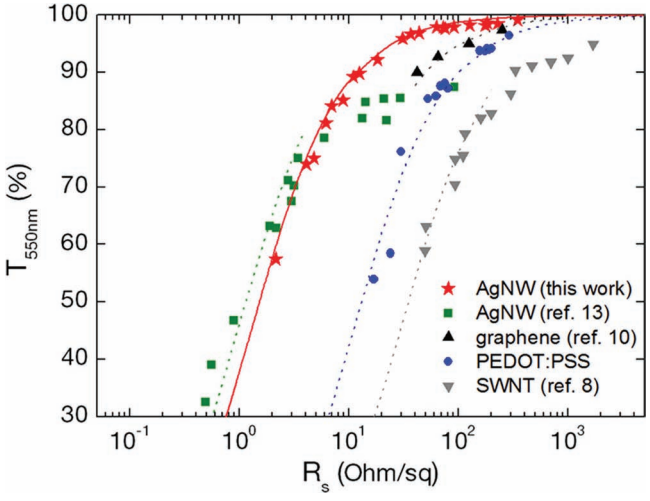

Figure 3. Plot of T (550 nm) vs. R_s for AgNW films. The data for the other nanostructured conducting materials were taken from the literature and replotted for comparison.

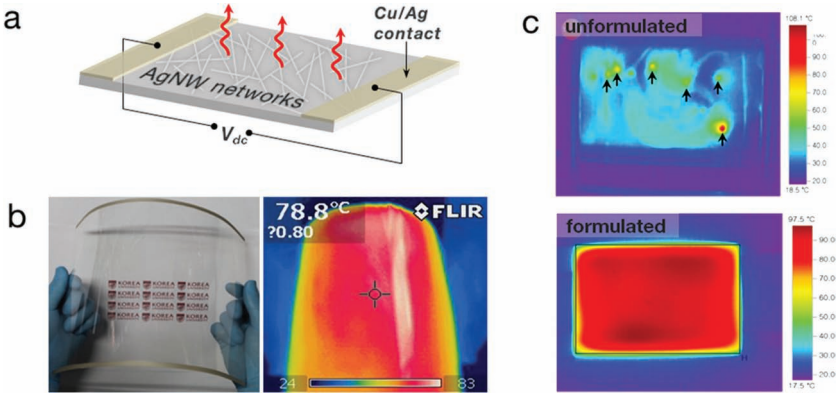

Figure 4. a) Schematic illustration of layouts for film heater with AgNW networks. b) A photograph and infrared image of the large-area AgNW-based film heater (250 mm × 200 mm), showing its mechanical flexibility. c) Infrared images of AgNW-based film heaters (50 mm × 75 mm) showing a hot spot due to the self-aggregated nanowires within the networks (upper image) and a uniform heat distribution (lower image).

with a high aspect ratio and the formation of uniformly interconnected nanowire networks.

To demonstrate its potential as an electrode for transparent heaters and the large-area scalability of our process, we constructed a macroscale AgNW-based film heater with dimensions of 250 × 200 mm^2 under a two-terminal side-contact configuration, as schematically illustrated in **Figure 4**a. The DC voltage was supplied by a power supply to the film heater through a copper or silver contact at the film edge and the temperature of the film was monitored using an IR thermometer. The temperature profile obtained from the IR thermometer was validated by a direct measurement with a thermocouple mounted on the top surface of the film. Figure 4b shows a photograph of the fabricated AgNW-based film heater and the corresponding infrared image, which shows a uniform heat distribution over the film under bending. We note that the failure to produce a uniformly interconnected network of AgNWs often causes "hot-spots" as shown in Figure 4c. Non-uniform networks would tend to have a broad distribution of wire-wire junction resistances resulting in localized heating at the point where the AgNWs are assembled into aggregated islands. In sharp contrast, the heat distribution of our AgNW network was anisotropic over the entire film, which was also confirmed by the thermocouple measured at different points (see the Supporting Information, Figure S1).

Figure 5a shows the time-dependent temperature profiles of the AgNW-based film heater with respect to the surface resistivity of the AgNW film. Under the application of the same input voltage (5 V), the maximum temperature at steady state increases as the surface resistivity of the film decreases, which suggests that the R_s value of the AgNW film should be less than 10 Ω sq^{-1} to afford the maximum temperature above 70 °C at an input voltage of 5 V. For AgNW films with R_s = 50 Ω sq^{-1}, an input voltage of at least 12 V is required for the temperature to reach 70 °C (Supporting Information, Figure S2-a). In the case of the AgNW film with R_s = 100 Ω sq^{-1}, input voltages more than 12 V are needed to reach this temperature (Supporting Information, Figure S2-b).

Figure 5b shows the temperature profiles of the film heater assembled with an AgNW film ($R_s \approx 10$ Ω sq^{-1}), which is plotted with respect to the input voltages (modulated from 3 to 7 V). When the input voltage was increased to 7 V, the film heater reached a temperature above 100 °C, confirming its operation at low input voltages. A high power at a low input voltage implies the efficient transduction of electrical energy into Joule heating, which may be attributed to the improved conductivity of the AgNW film. The response time, which is defined as the time required to reach the steady-state temperature, is one of the key factors for evaluating the performance of film heaters. Regardless of the input voltages, the steady-state temperature of the film heater was reached within 60 s, demonstrating the fast response of the device. Considering that a film heater based on large-scale CVD-grown doped graphene (90 mm × 90 mm) reached only 55 °C under an input voltage of 30 V,[24] our AgNW-based device outperforms other nanostructured material-based film heaters, and thus will be useful for applications that require fast temperature switching with low input voltages. For

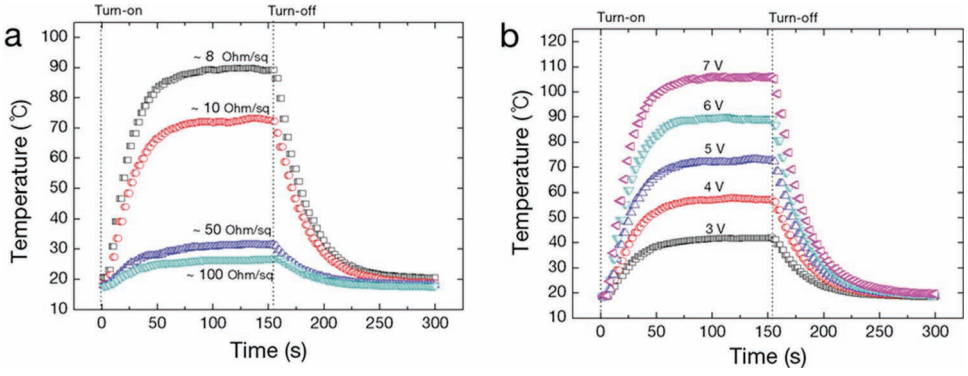

Figure 5. a) Time-dependent temperature profiles of AgNW-based film heaters (50 mm × 75 mm) with respect to the surface resistivity of the AgNW films. b) Temperature profiles of the AgNW film heater ($R_s \approx 10$ Ω sq^{-1}) under its operation at different input voltages.

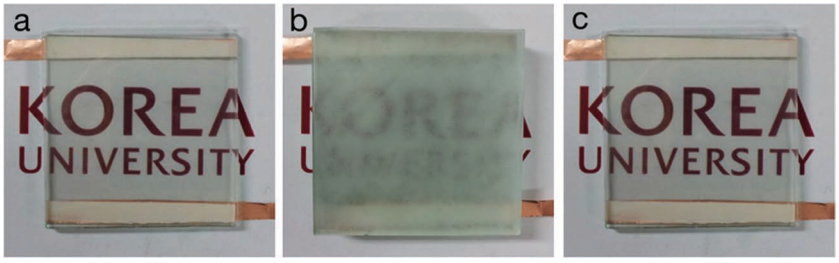

Figure 6. Defrosting test results of a AgNW film heater: a) before and b) after frost formation. c) After operation of the film heater at 12 V.

example, an input voltage less than 12 V is preferably required for automobile window defrosters, and thus a AgNW-based film heater may be a good option.

To demonstrate further its potential as an efficient defroster, a defrost test was performed with the AgNW-based film heater (**Figure 6**). For this test, a AgNW film was attached to a glass substrate and put in a refrigerator for 30 min to allow frost to form on the entire AgNW film. With the film heater operating at 12 V, the frost on the surface was completely removed within 60 s, makes the symbol marks in the background clearly visible. Therefore, these solution-processed AgNW-based films may enable new applications such as inexpensive coatings for highly transparent large-scale film heaters.

Another advantage of our AgNW-based film heater is the mechanical robustness against adhesion and bending, since the AgNWs are firmly anchored on PET films, afforded by the stacked clay platelets. For this purpose, we investigated the effect of bending on the electrical resistance of the AgNW film with $R_s \approx 10\ \Omega\ sq^{-1}$ and $T \approx 90\%$. No obvious increase in $\Delta R/R_0$ was observed after a standard tape test or when the AgNW films were bent to a curvature of 10 mm, as shown in **Figure 7**a. Unlike an ITO-based film heater, the absence of cracking or tearing suggests high levels of mechanical flexibility of the AgNW-based film heaters, which is evidenced by the repeated bending test of the film heater under the application of the input voltage (Figure 7b).

3. Conclusions

In summary, we have presented a method of preparing highly transparent and flexible electrodes based on solution-processed AgNW networks. With the utilization of exfoliated clays as a key element for improving solution and coating properties of AgNW inks, the nanowire networks prepared by this method are efficiently interconnected with an improved spatial uniformity. This renders the AgNW film a relatively high figure-of-merit (with σ_{dc}/σ_{op} value of >300) very close to that of ITO, with optimally balanced optical transmittance and surface resistivity in the technically relevant regime. Advantages of this solution-processed AgNW film include mechanical flexibility and scalability to large areas in a roll-to-roll system. The AgNW films demonstrated here possess attractive features for both conventional and emerging applications of transparent flexible electrodes for large-area flexible electronic devices.

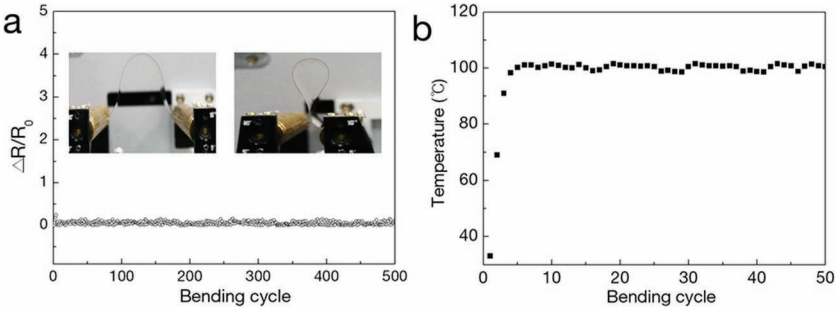

Figure 7. a) Resistance change of AgNW-coated film under bending testing. The inset photo shows the bending process. b) Variation in temperature of a AgNW-based film heater under repeated bending cycles.

4. Experimental Section

Solution-Based Synthesis of Silver Nanowires: Silver nanowires (AgNWs) were synthesized using the modified polyol method. Briefly, 4.17 g of poly(vinyl pyrrolidone) (PVP) ($M_w \approx 55\ 000\ g\ mol^{-1}$) and 0.13 g of 1-butyl-3-methylimidazolium chloride (BMIM-Cl) were dissolved in 440 mL of ethylene glycol (EG). Under stirring, the reaction mixture was heated to 90 °C. After the temperature of the reaction mixture was stabilized, $AgNO_3$ precursor solution (in EG, 1 M, 21 mL) was added dropwise into the mixture at a constant rate (1.3 mL h^{-1}) over a period of 20 h. The reaction mixture was allowed to react for a further 4 h and cooled to room temperature. The nanowires were washed with ethanol and collected by centrifugation at 4000 rpm for 30 min. This was repeated three times to remove the residual solvent (i.e., ethylene glycol) and chemical agents (i.e., PVP and BMIM-Cl).

Preparation of AgNW-Coated Films: The as-synthesized AgNWs were re-dispersed in deionized water (5 mg mL^{-1}) with dispersing agent (polyethylene glycol sorbitan monolaurate, 0.2 mg mL^{-1}). Separately, synthetic clay made of nanometer-sized discotic platelets (Laponite RDS) was added to deionized water with a concentration of 2.5 mg mL^{-1}, and exfoliated under continuous stirring at 60 °C for 12 h. A slightly increasing solution viscosity was typically observed when the exfoliated clay was dispersed as separate clay platelets. In case further control of the solution viscosity was required, a certain amount of hydroxypropyl methylcellulose was added into the solution. Then, the clay dispersion was added into the AgNW dispersion to give a AgNW/clay ratio of 2/1 by weight. The as-formulated AgNW ink was coated onto 125 μm-thick optical grade PET film using a wire-wound rod and dried in an oven at 100 °C for 2 min. The film thickness could be controlled by tuning the ink volume in the groove space of the wire-wound rod and the concentration of the ink. This procedure allowed the large-scale coating of AgNW networks and can be easily scaled by using slot die or gravure coating.

AgNW-Based Film Heaters: A large-scale AgNW-based film heater (50 mm × 75 mm and 250 mm × 200 mm) was made in a two-terminal side-contact configuration. The DC voltage was supplied by a power supply (Keithley 2400) to the film heater through a copper or silver contact at the film edge. The temperature of the film was measured using an IR thermal imager (Testo 880) and the thermocouple was mounted on the top surface of the film. For the defrost test, the AgNW film with a surface resistivity of 50 Ω sq^{-1} was prepared and attached to the glass substrate. The film was put in a refrigerator for 30 min to induce frost formation, after which an input voltage of 12 V was applied to the film heater.

Characterization: SEM measurements were made using a Hitachi S-4800 field emission scanning electron microscope. All of the LSM images were taken using an Olympus OLS 4000 3D measuring laser microscope. The optical transmission spectra were recorded using a Cary Varian 5000 UV–vis–NIR spectrophotometer, with a PET film used as the reference. The total transmission measurements were taken on Otsuka MCPD 3700 with an integrating sphere. Surface-resistivity measurements were made using a standard four-point probe method using an AIT CMT-100MT instrument. The bending test was carried out with lab-made apparatus with software recording film resistance and cycle number.

Supporting Information

Supporting Information is available from the Wiley Online Library or from the author.

Acknowledgements

We appreciate financial support from SOLOE Tech, Co. Ltd, Korea.This article was modified after online publication. The film dimensions were added to the captions of figures 4 and 5 and details missing from the Experimental Section were added.

Received: July 18, 2012
Published online: October 15, 2012

[1] A. Kumar, C. Zhou, *ACS Nano* **2010**, *4*, 11–14.
[2] D. S. Hecht, L. Hu, G. Irvin, *Adv. Mater.* **2011**, *23*, 1482–1513.
[3] S. Pang, Y. Hernandez, X. Feng, K. Müllen, *Adv. Mater.* **2011**, *23*, 2779–2795.
[4] S. Kirchmeyer, K. J. Reuter, *Mater. Chem.* **2005**, *15*, 2077–2088.
[5] A. G. MacDiarmid, *Angew. Chem. Int. Ed.* **2001**, *40*, 2581–2590.
[6] Z. Wu, Z. Chen, X. Du, J. M. Logan, J. Sippel, M. Nikolou, K. Kamaras, J. R. Reynolds, D. B. Tanner, A. F. Hebard, *Science* **2004**, *305*, 1273–1276.
[7] E. M. Doherty, S. De, P. E. Lyons, A. Shmeliov, P. N. Nirmalraj, V. Scardaci, J. Joimel, W. J. Blau, J. J. Boland, J. N. Coleman, *Carbon* **2009**, *47*, 2466–2473.
[8] V. Scardaci, R. Coull, J. N. Coleman, *Appl. Phys. Lett.* **2010**, *97*, 023114.
[9] X. S. Li, Y. W. Zhu, W. W. Cai, M. Borysiak, B. Y. Han, D. Piner, R. D. Chen, L. Colombo, R. S. Ruoff, *Nano Lett.* **2009**, *9*, 4359–4363.
[10] S. Bae, H. Kim, Y. Lee, X. F. Xu, J. S. Park, Y. Zheng, J. Balakrishnan, T. Lei, H. R. Kim, Y. I. Song, Y. J. Kim, K. S. Kim, B. Ozyilmaz, J. H. Ahn, B. H. Hong, S. Iijima, *Nat. Nanotechnol.* **2010**, *5*, 574–578.
[11] G. Eda, G. Fanchini, M. Chhowalla, *Nat. Nanotechnol.* **2008**, *3*, 270–274.
[12] M. G. Kang, M. S. Kim, J. S. Kim, L. J. Guo, *Adv. Mater.* **2008**, *20*, 4408–4413.
[13] S. De, P. J. King, P. E. Lyons, U. Khan, J. N. Coleman, *ACS Nano* **2010**, *4*, 7064–7072.
[14] S. De, T. M. Higgins, P. E. Lyons, E. M. Doherty, P. N. Nirmalraj, W. J. Blau, J. J. Boland, J. N. Coleman, *ACS Nano* **2009**, *3*, 1767–1774.
[15] L. Hu, H. S. Kim, J. Lee, P. Peumans, Y. Cui, *ACS Nano* **2010**, *4*, 2955–2963.
[16] H. Wu, L. Hu, M. W. Rowell, D. Kong, J. J. Cha, J. R. McDonough, J. Zhu, Y. Yang, M. D. McGehee, Y. Cui, *Nano Lett.* **2010**, *10*, 4242–4248.
[17] V. Scardaci, R. Coull, P. E. Lyons, D. Rickard, J. N. Coleman, *Small* **2011**, *7*, 2621–2628.
[18] W. Gaynor, J. Lee, P. Peumans, *ACS Nano* **2010**, *4*, 30–34.
[19] Z. Yu, L. Li, Q. Zhang, W. Hu, Q. Pei, *Adv. Mater.* **2011**, *23*, 4453–4457.
[20] L. Li, Z. Yu, W. Hu, C. Chang, Q. Chen, Q. Pei, *Adv. Mater.* **2011**, *23*, 5563–5567.
[21] X. Zeng, Q. Zhang, R. Yu, C. Lu, *Adv. Mater.* **2010**, *22*, 4484–4488.
[22] C. Kim, S. Cha, S. C. Kim, M. Song, J. Lee, W. S. Shin, S. Moon, J. H. Bahng, N. A. Kotov, S. Jin, *ACS Nano* **2011**, *5*, 3319–3325.
[23] Y. Yoon, J. Song, D. Kim, J. Kim, J. Park, S. Oh, C. Han, *Adv. Mater.* **2007**, *19*, 4284–4287.
[24] J. Kang, H. Kim, K. S. Kim, S. Lee, S. Bae, J. Ahn, Y. Kim, J. Choi, B. H. Hong, *Nano Lett.* **2011**, *11*, 5154–5158.
[25] D. Sui, Y. Huang, L. Huang, J. Liang, Y. Ma, Y. Chen, *Small* **2011**, *7*, 3186–3192.
[26] Y. Sun, Y. Yin, B. T. Mayers, T. Herricks, Y. Xia, *Chem. Mater.* **2002**, *14*, 4736–4745.
[27] Y. Sun, B. Gates, B. Mayers, Y. Xia, *Nano Lett.* **2002**, *2*, 165–168.
[28] T. Y. Kim, W. J. Kim, S. H. Hong, J. E. Kim, K. S. Suh, *Angew. Chem. Int. Ed.* **2009**, *48*, 3806–3809.
[29] B. Ruzicka, E. Zaccarelli, L. Zulian, R. Angelini, M. Sztucki, A. Moussaid, T. Narayanan, F. Sciortino, *Nat. Mater.* **2011**, *10*, 56–60.
[30] S. M. Liff, N. Kumar, G. H. McKinley, *Nat. Mater.* **2007**, *6*, 76–83.
[31] R. D. Deegan, O. Bakajin, T. F. Dupont, G. Huber, S. R. Nagel, T. A. Witten, *Nature* **1997**, *389*, 827–829.
[32] W. Han, Z. Lin, *Angew. Chem. Int. Ed.* **2012**, *51*, 1534–1546.